# Histidine adsorption onto modified montmorillonite under prebiotic chemistry conditions: a thermodynamic and kinetic study

Rafael Block Samulewski[1], Regiane Tamires Damasceno Guimarães[2] and Dimas Augusto Morozin Zaia[2] (iD)

[1]Universidade Tecnológica Federal do Paraná, Campus Apucarana, Centro, 86812460 Apucarana, PR, Brazil and [2]Laboratório de Química Prebiótica-LQP, Departamento de Química-CCE, Universidade Estadual de Londrina – UEL, CEP 86812-460 Londrina, PR, Brazil

## Research Article

### Abstract

The origin of life from inanimate matter is still an open question, and our knowledge is still very limited. In this sense, prebiotic chemistry seeks to study and understand how chemical reactions may have contributed to the origin of life. Minerals are of great relevance to prebiotic chemistry, as they may have preconcentrated precursors of biomolecules or biomolecules from diluted solutions, provided protection for biomolecules against UV radiation and hydrolysis, catalysing their reactions and played the role of a primitive genetic code. Montmorillonite, a prebiotic mineral, was shown to be able to adsorb adenine and later also histidine. In addition, histidine adsorption did not displace adenine from the montmorillonite. Kinetic experiments showed that using a whole period of time (7 days) it was not possible to adjust the data to any mathematical kinetic model. Thus, the data were separated into four different adsorption ranges: range 1 (0–60 min), range 2 (60–4320 min), range 3 (4320–7200 min) and range 4 (7200–10 080 min). Range 1 showed adsorption that was too fast, meaning no variations in the adsorption data, and the data of range 3 did not fit in any model used in this work. Thus, range 2 (60–4320 min) and range 4 (7200–10 080 min) were analysed. The adsorption kinetics of histidine adsorption indicated two reaction steps, a quick step (60–4320 min), following the pseudo-first-order model, followed by a slower step (7200–10 080 min) of the pseudo-second order. With these results, isotherms were constructed with times of 1 h and 7 days. The results of the quick step (1 h) showed a reaction that was not thermodynamically favoured. For this time range, Gibbs energy values obtained ranged between 5 and 10 kJ mol$^{-1}$ at temperatures of 20, 35 and 50°C, and the adsorption occurred due to the balance shift of increase in histidine concentrations. The isotherms of the slow step (7 days) presented negative values, showing a more favourable reaction with Gibbs energy values ranging between −5 and −11 kJ mol$^{-1}$. The mathematical modelling of the data indicates that seawater ions are crucial in the adsorption process. Thus, the study provided essential information for prebiotic chemistry, showing that time and the reaction medium should always be taken into account.

## Introduction

Since the beginning of time, man has wondered how life on Earth came about. Prebiotic chemistry studies reactions and processes that may have contributed to the origin of life. These studies are performed under conditions that existed 3.8 billion years ago, mainly reactions with gas mixtures, reactions in the solid state, hydration and dehydration cycles, and reactions in aqueous and hydrothermal solutions (Lazcano and Miller, 1996; Schoonen et al., 2004; Holm and Andersson, 2005). Bernal suggested that minerals may have played an important role in the prebiotic era, proposing that they could have overcome the problem of diluting molecules in primitive seas. Minerals could also have provided protection for molecules against degradation by hydrolysis and ultraviolet radiation, as well as functioning as catalysts for biopolymers and forming a genetic pre-code (Bernal, 1951). Among the minerals that may be associated with the origin of life, montmorillonite is among the most widely used for prebiotic experiments (Lahav and Chang, 1976; Lahav, 1994; Lambert, 2008; Zaia, 2012). In addition, montmorillonite could be found on Earth before life arose on it (Hazen et al., 2008).

Histidine could be synthesized in several different ways, such as redox-neutral atmospheres (Plankensteiner et al., 2006), hydrothermal vents (Shen et al., 1990) and NH$_3$/HCN/NH$_2$CH mixtures (Lowe et al., 1963; Ferris et al., 1978; Ferris and Hagan, 1984). Adenine could be synthesized in environments simulating interstellar medium (Bera et al., 2017) and aqueous solutions of HCN (Roy et al., 2017), as well as being found in meteorites (Stoks and

Schwartz, 1979; Martins, *et al.*, 2008). Since histidine, adenine and montmorillonite existed on the prebiotic Earth, interaction among them occurred.

The adsorption would be the first step of a series of processes; if the adsorption does not occur the other processes will not occur. Minerals have a charged surface and can therefore adsorb organic molecules, concentrating them and providing a catalytic environment for the formation of complex molecules, such as peptides/proteins, and also self-replicating informational molecules, such as nucleotides and primitive RNA (Bernal, 1951; Rao *et al.*, 1980; Fripiat, 1984; Ferris, 1993). Based on the hypothesis of Bernal (1951), several studies were and are being carried out that involve the formation of amino acids and their condensation for peptide formation, as well as studies involving nitrogenous bases adsorbed on minerals. These studies are relevant to prebiotic chemistry since the majority of the reactions of current living beings involve these biomolecules (Darnell *et al.*, 1990).

As pointed out above, since adsorption is the first and most important step for the emergence of life, many works on adsorption, both amino acids and nitrogenous bases, have been published. For amino acids adsorption on minerals, some examples are highlighted: clays (Jackson, 1971; Paecht-Horowitz, 1977; Aufdenkampe *et al.*, 2001; Ding and Henrichs, 2002; Benetoli *et al.*, 2007; Jaber *et al.*, 2014); hematite, magnetite and ferrihydrite (Ben-Taleb *et al.*, 1994; Vieira *et al.*, 2011) silica, quartz and sand (Basiuk and Gromovoy, 1996; Basiuk, 2002; Zaia *et al.*, 2002; Churchill *et al.*, 2004); river and sea sediments (Henrichs and Sugai, 1993; Montluçon and Lee, 2001; Ding and Henrichs, 2002); calcite, albite and hydroxyapatite (Tanaka *et al.*, 1989; Churchill *et al.*, 2004); zeolites (Carneiro *et al.*, 2011a); goethite (Farias *et al.*, 2016); FeS$_2$ (Suzuki *et al.*, 2018) and rutile (Lee *et al.*, 2014). For purine and pyrimidine adsorption, there are also some examples from the literature: clays (Lahav and Chang, 1976; Perezgasga *et al.*, 2005; Winter and Zubay, 1995; Benetoli *et al.*, 2008; Carneiro *et al.*, 2011b); and zeolites (Baú *et al.*, 2012; Anizelli *et al.*, 2015, 2016; Villafañe-Barajas *et al.*, 2018).

In general, prebiotic chemistry experiments use up to 24 h to study the adsorption of molecules onto minerals. In the present work, the adsorption of histidine onto montmorillonite was studied over 7 days. The kinetic and thermodynamic parameters of the adsorption of histidine onto montmorillonite with and without pre-adsorbed adenine were obtained. In addition, the effect of salts of the artificial seawater on the adsorption of histidine onto montmorillonite was studied.

## Materials and methods

### Materials

All compounds were used without further purification.

### Montmorillonite

Montmorillonite-KSF (CAS-1318-93-0, Acros Organics) was saturated with sodium chloride as follows: 100 mg of montmorillonite-KSF was dispersed in 50 ml of saturated NaCl (360 mg l$^{-1}$) solution. The dispersion was under stirring for 24 h, after which the sample was filtered and washed three times with ultrapure water. Then the sample was dried at 40°C. Ultrapure water (U) was obtained from Merk Millipore® (Milli-Q).

### Seawater 4.0 Gy (SW)

Artificial seawater 4.0 Gy (SW) was prepared as described by Zaia (2012). The artificial seawater has the following chemical composition in g l$^{-1}$: Na$_2$SO$_4$ (0.271), MgCl$_2$·6H$_2$O (0.500), CaCl$_2$·2H$_2$O (2.50), KBr (0.05), K$_2$SO$_4$ (0.400) and MgSO$_4$ (15.00). This artificial seawater is called 100% and has a pH ≈ 6.0. Subsequently, this solution was diluted to a 10% solution.

### Mineral modification

The mineral modification was carried out at 30°C. A total of 5 g of montmorillonite and a solution of 250 ml of adenine (720 µg ml$^{-1}$) dissolved in ultrapure water were mixed in an Erlenmeyer flask. The same experiment was repeated using a solution of adenine (720 µg ml$^{-1}$) dissolved in artificial seawater 4.0 Gy 10%. All suspensions were stirred for 1 h. After that, the minerals were filtered, frozen and lyophilized for the use in the adsorption of histidine; two different sorbents were obtained: montmorillonite modified with adenine in ultrapure water (MAUW) and montmorillonite modified with adenine in seawater 4.0 Gy 10% (MASW). We also have pure montmorillonite (M).

## Methods

### Fourier transform infrared spectroscopy – FTIR

For all samples, the FTIR spectra from 4000 to 400 cm$^{-1}$ were obtained using a Bruker Vertex 70 spectrophotometer with attenuated total reflectance (ATR). A resolution of 2 cm$^{-1}$ and 16 scans were used to obtain all the spectra.

### UV spectrophotometry

A spectrum SP-2000UV UV–vis spectrophotometer was used to quantify adenine and histidine, at wavelengths of 260 and 212 nm, respectively. Standard curves of adenine and histidine were used for the quantification. The amount of histidine or adenine adsorbed onto the minerals was calculated by using the following equation:

$$C_{adsorbed\,(\mu g)} = (C_{initial} - C_{solution})$$
$$\text{where } C_{solution} = [(C_{initial})(Abs_{sample}/Abs_{initial})] \tag{1}$$

### Determination of pH at point of zero charge (pH$_{pzc}$)

The pH$_{pzc}$ of montmorillonite samples was determined from its suspension. In two 1.5 ml Eppendorf tubes, 50 mg of mineral and 250 µl of ultrapure water were added to the first tube and 250 µl of KCl 1.0 mol l$^{-1}$ solution to the second tube. Then, the tubes were shaken for 30 min, followed by resting for 24 h. The pH reading was performed on a pH meter, ion model pHB 500 and the pH$_{pzc}$ of the minerals was determined using equation (2) (Uehara, 1979).

$$pH_{pzc} = 2\,pH_{KCl} - pH_{H_2O} \tag{2}$$

### The pH variation study

The pH variation studies were performed in triplicate, at a controlled temperature of 25°C and constant stirring for 24 h. The histidine solution was prepared in different pH ranges (2.00; 3.00; 4.00; 5.00; 6.00; 7.00 and 8.00), using sodium hydroxide solution (0.1 mol l$^{-1}$) and hydrochloric acid (0.1 mol l$^{-1}$). In 15 ml falcon tubes, 50 mg of mineral and 5 ml of histidine (720 µg ml$^{-1}$) solution were added. Experiments were carried

**Table 1.** Non-linear forms of the adsorption kinetics and isotherm models

| Kinetic equations | | |
|---|---|---|
| **Kinetic models** | **Equations** | **Variables** |
| Pseudo-first order | $q_t = q_e e^{-k_1^t}$ | $q_t$ quantity adsorbed (mol g$^{-1}$) at time $t$; $q_e$ quantity adsorbed (mol g$^{-1}$) at time equilibrium; $k_1$ rate constant (min$^{-1}$); $k_2$ rate constant (g mg$^{-1}$ min$^{-1}$); $t$ time (min) |
| Pseudo-second order | $q_t = q_e/(1 + k_2 t q_e)$ | |
| **Adsorption isotherms** | | |
| **Isotherm models** | **Equations** | **Variables** |
| Langmuir | $Q_e = (Q_{max} K_L C_{eq})/(1 + K_L C_{eq})$ | $Q_e$ equilibrium amount adsorbed (mg g$^{-1}$); $C_{eq}$ concentration at equilibrium (mg l$^{-1}$); $Q_{max}$ maximum adsorption capacity (mg g$^{-1}$); $K_L$ Langmuir constant; $K_F$ Freundlich constant; $n$ Freundlich's heterogeneity factor |
| Freundlich | $Q_e = K_F C_{eq}^n$ | |
| Langmuir–Freundlich/SIPS | $Q_e = (Q_{max} K_L C_{eq}^n)/(1 + K_L C_{eq}^n)$ | |

**Table 2.** Linear system representing an individual contribution of possible interactions A, B, C and D of all isotherms and results for system components contribution

| Sample | $\Delta H_{exp} =$ | $\Delta S_{exp} =$ | Calc. | 0–60 min | | 0–10 080 min | |
|---|---|---|---|---|---|---|---|
| | | | | H | S | H | S |
| M-UW | HA | SA | | | | | |
| M-SW | HA + HB | SA + SB | A | −2.3 | −26.8 | 15.41 | 18.62 |
| MAUW-UW | HA + HC | SA + SC | B | 8.2 | 17.5 | −9.90 | 29.48 |
| MAUW-SW | HA + HB + HC | SA + SB + SC | C | 0.9 | −6 | −0.70 | 4.1 |
| MASW-UW | HA + HC + HD | SA + SC + SD | D | 16.3 | 54 | 16.60 | 54.72 |
| MASW-SW | HA + HB + HC + HD | SA + SB + SC + SD | | | | | |

M-SW = histidine dissolved in seawater 4.0 (10%), and adsorbed on montmorillonite; MAUW-UW = histidine dissolved in ultrapure water, and adsorbed on modified montmorillonite with adenine in ultrapure water; MAUW-SW– histidine dissolved in seawater 4.0 (10%), and adsorbed on montmorillonite modified with adenine in ultrapure water; MASW-UW – histidine dissolved in ultrapure water, and adsorbed on montmorillonite modified with adenine in seawater 4.0 (10%); MASW-SW – histidine dissolved in seawater 4.0 (10%), and adsorbed on montmorillonite modified with adenine in seawater 4.0 (10%). $\Delta H_{exp}$ = experimental enthalpy; $\Delta S_{exp}$ = experimental entropy.

out with ultrapure water (UW) and seawater 4.0 Gy 10% (SW) with minerals M, MUW and MSW.

### Adsorption kinetics of histidine onto montmorillonites

Kinetic studies of histidine adsorption on the different minerals (M, MAUW and MASW) were performed in triplicate, at 25°C and constant agitation, for 168 h. A total of 10 mg of mineral and 2.0 ml of histidine solution (720 μg ml$^{-1}$) were added to Eppendorf tubes. The pH of the samples was from 4.00 to 5.00. Aliquots were removed at certain times; these aliquots were used to determine the adsorption of histidine onto minerals. The experiments were carried out using unmodified mineral or modified with adenine, as well as varying the solution of histidine in ultrapure water (UW) and seawater 4.0 Gy (SW) for each mineral.

### Adsorption isotherms

The adsorption isotherms were performed in triplicate, with a controlled temperature. Histidine was dissolved in ultrapure water (UW) and seawater (SW) at different concentrations (20, 40, 60, 80, 100, 200, 300, 400, 500, 600, 700, 800, 900 and 1000 μg ml$^{-1}$). For the assay, 1 ml of the solution was added to 10 mg of the mineral. Each tube was left in a thermostatic bath for 1 h and then centrifuged for 15 min at 6000 rpm, after which the mineral and supernatant were stored separately for further analysis. The experiments were repeated for the modified minerals, all in triplicate, at three temperatures, 20, 35 and 50°C, respectively. For isotherms performed in 168 h,

the same procedures were performed, changing only the time the tubes were left in a thermostatic bath.

### Mathematical modelling

For the modelling of the kinetic and adsorption isotherm experiments, non-linear regression methods were used (Table 1). For the kinetic experiments, the pseudo-first-order and pseudo-second-order models were used, and for the adsorption isotherm experiments, the Langmuir, Freundlich and Langmuir–Freundlich (SIPs) models were used (Foo and Hameed, 2010). Thermodynamic data of system components A, B, C and D contributions were calculated using a simple linear system in order to minimize the theoretical/experimental deviation. The only fixed parameter was parameter 'A' and the others were calculated using the linear system (Table 2) with the $\Delta H$ and $\Delta S$ results obtained experimentally.

### Seawater ion quantification

The quantification analyses of sodium, potassium and calcium ions in 4.0 Gy seawater were performed using an AJ Micronal Flame Photometer – B462. For the quantification of sulphate in 4.0 Gy seawater, a gravimetric method was used, which is based on the precipitation of barium sulphate by slowly adding a barium chloride solution to a sulphate solution (Zenebon et al., 2008). To quantify the magnesium ions, the complexation titration technique was used. The magnesium concentration was determined by subtracting the calcium concentration obtained from the flame photometer (Zenebon et al., 2008).
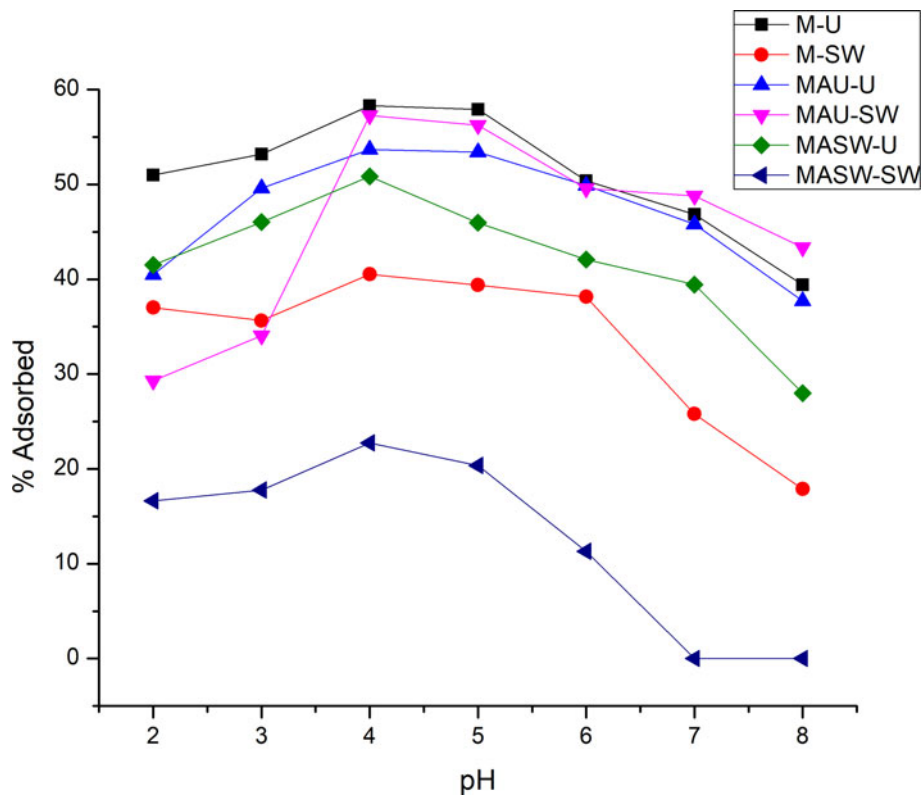
Fig. 1. Adsorption of histidine onto different montmorillonites and different pHs. M-UW = histidine dissolved in ultrapure water, and adsorbed on montmorillonite; M-SW = histidine dissolved in seawater 4.0 (10%), and adsorbed on montmorillonite; MAUW-UW = histidine dissolved in ultrapure water, and adsorbed on modified montmorillonite with adenine in ultrapure water; MAUW-SW- Histidine dissolved in seawater 4.0 (10%), and adsorbed on montmorillonite modified with adenine in ultrapure water; MASW-UW – histidine dissolved in ultrapure water, and adsorbed on montmorillonite modified with adenine in seawater 4.0 (10%); MASW-SW – histidine dissolved in seawater 4.0 (10%), and adsorbed on montmorillonite modified with adenine in seawater 4.0 (10%) (Experimental parameters: [Histidine]$_{initial}$ = 720 mg l$^{-1}$; time = 60 min; Temp. = 25°C.).
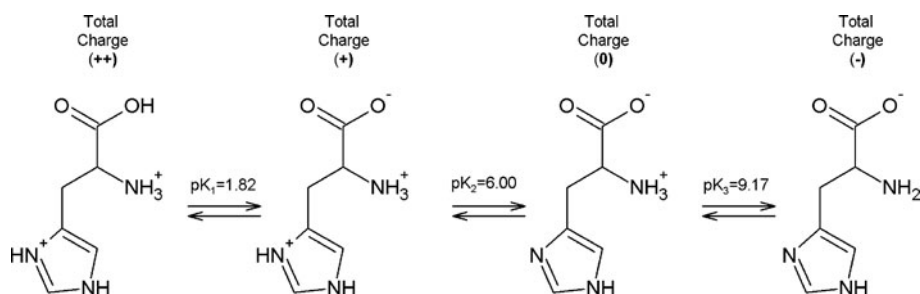


Fig. 2. Schematic histidine total charge and respective pKa values.

## Results and discussion

### Adsorption of adenine

Montmorillonite modification involved the adsorption of adenine onto it as described in the methodology. The pH of the solution before and after adsorption was between 4.00 and 5.00. The results showed that approximately 89% of the adenine dissolved in ultrapure water and seawater 4.0 Gy were adsorbed by the montmorillonite. At pH between 4.00 and 5.00, adenine is positively charged (pK$_{a1}$ < 1.0; pK$_{a2}$ = 4.1; and pK$_{a3}$ = 9.8), and montmorillonite is negatively charged (pH$_{pzc}$: M = 0.54; MAUW = 0.59; and MASW = 1.12). These opposite charges result in high adsorption through electrostatic attraction between adenine and the negative montmorillonite surface (Benetoli *et al.*, 2008; Carneiro *et al.*, 2011a; Villafañe-Barajas *et al.*, 2018).

### Effect of pH on the histidine adsorption onto montmorillonite

In order to better understand and define the best pH for histidine adsorption, experiments with pH variation were performed (Fig. 1). The best pH range for adsorption was between 4.00

and 5.00 (Fig. 1). The pKa values for histidine aid understanding of a better response to adsorption of histidine at a low pH and that the pH in a basic medium does not show considerable adsorption (Fig. 2). According to this, histidine at pH between 4.00 and 5.00 is positively charged and montmorillonite is negatively charged. Therefore, electrostatic forces favoured the adsorption of histidine onto montmorillonite. Similar results have been described by Hedges and Hare using $10^{-6}$ mol l$^{-1}$ histidine solution in ultrapure water (Hedges and Hare, 1987). According to the authors, approximately 50% of the histidine adsorbed onto montmorillonite and kaolinite. The authors attributed the adsorption to the opposite charge attraction between the mineral and amino acid. The highest histidine adsorption was obtained by dissolving it in ultrapure water and using pure montmorillonite (M) as a sorbent (Fig. 1). The lowest histidine adsorption occurred when it was dissolved in artificial seawater 4.0 Gy 10% and montmorillonite modified with adenine in seawater 4.0 Gy 10% (MASW) was used as a sorbent (Fig. 1). These data show that salts of seawater interfere with histidine adsorption, meaning they share the same sites of montmorillonite for their adsorption. It should be noted that Mg$^{2+}$ and SO$_4^{2-}$ were adsorbed by
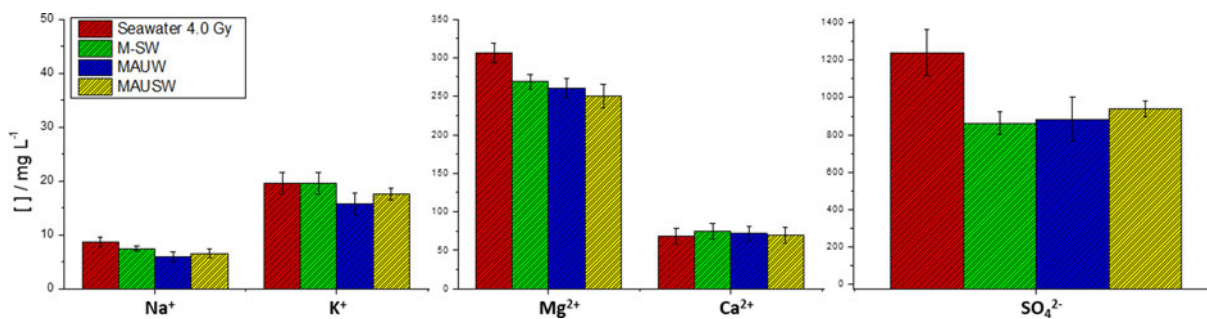
**Fig. 3.** Bar graph of seawater 4.0 Gy ions concentration (mg l$^{-1}$) before (red bar) and after 1 h of histidine adsorption essays. Bars colour: green = M, ciano = MAUW and yellow =⍰⍰⍰MASW experiments, M-SW = histidine dissolved in seawater 4.0 (10%), and adsorbed on montmorillonite; MAUW-SW – histidine dissolved in seawater 4.0 (10%), and adsorbed on montmorillonite modified with adenine in ultrapure water; MASW-SW – histidine dissolved in seawater 4.0 (10%), and adsorbed on montmorillonite modified with adenine in seawater 4.0 (10%) (Experimental parameters: [Histidine]$_{initial}$ = 720 mg l$^{-1}$; time = 60 min; Temp. = 25°C.).
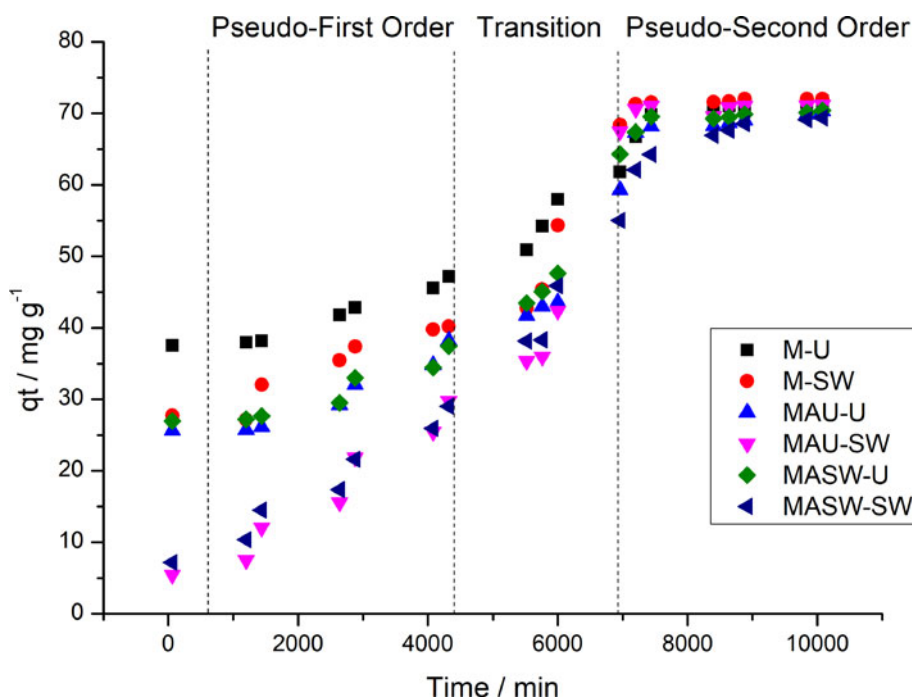


**Fig. 4.** Histidine adsorption onto mineral samples and solutions at different times (Hardy, 1985). M-UW = histidine dissolved in ultrapure water, and adsorbed on montmorillonite; M-SW = histidine dissolved in seawater 4.0 (10%), and adsorbed on montmorillonite; MAUW-UW = histidine dissolved in ultrapure water, and adsorbed on modified montmorillonite with adenine in ultrapure water; MAUW-SW – histidine dissolved in seawater 4.0 (10%), and adsorbed on montmorillonite modified with adenine in ultrapure water; MASW-UW – histidine dissolved in ultrapure water, and adsorbed on montmorillonite modified with adenine in seawater 4.0 (10%); MASW-SW – histidine dissolved in seawater 4.0 (10%), and adsorbed on montmorillonite modified with adenine in seawater 4.0 (10%).

montmorillonite (Fig. 3). Farias *et al.* (2014) and Villafañe-Barajas *et al.* (2018) also observed a decrease in the adsorption of amino acids and nucleic acid bases onto montmorillonite due to cations of seawater, respectively. In addition, for all experiments, histidine did not displace adenine from clay.

### Histidine adsorption kinetic onto montmorillonite

Adsorption kinetics of histidine showed that the amino acid adsorption occurs for up to 7 days after the reaction begins (Fig. 4). The mathematical modelling of the data did not show kinetic adjustment when all data were used for the whole period of time. Therefore, using mathematical modelling to separate adsorption data, it was possible to separate the kinetic experiment results into four different adsorption ranges: range 1 = 0–60 min; range 2 = 60–4320 min; range 3 = 4320–7200 min; and range 4 = 7200–10 080 min (Fig. 4).

Range 1 did not show variations in the adsorption data, signifying quick adsorption (Fig. 4). This quick adsorption may have occurred due to electrostatic forces arising from the negative

charge of the mineral at the interlayer and the positive histidine charge (Li *et al.*, 2010). With respect to range 1, it is possible to observe that seawater 4.0 Gy cations decrease the initial percentage adsorption caused by initial competition between histidine and seawater cations. As pointed out above, Farias *et al.* (2014) and Villafañe-Barajas *et al.* (2018) also observed the same effect for the adsorption of amino acids and nucleic acid bases onto montmorillonite, respectively. As the adsorption data for the time range from 0 to 60 min were the same for all experiments, there is no mathematical model to describe this process.

For Range 2, the pseudo-first-order model showed the best fit (Table 3). In addition, the adsorption reaction was faster when carried out in seawater (Table 3). For pre-adsorbed adenine samples and seawater medium, although initial adsorption is less, the adsorption reaction is faster and there is an increase in the amount adsorbed at equilibrium (Table 3). The pseudo-first-order kinetic model usually applies to the beginning of the adsorption process, where the concentration of free sites in the adsorbent is much higher than the occupied sites (Largitte and Pasquier, 2016). Thus, at the beginning of the adsorption experiments,

**Table 3.** Kinetic parameters for histidine adsorption onto different minerals on the selected time range

| | Kinetic parameters | | | | | |
|---|---|---|---|---|---|---|
| | Pseudo-first order Range 2 60–4320 min | | | Pseudo-second order Range 4 7200–10 080 min | | |
| Sample | $k_1$ (min$^{-1}$) | $q_e$ (mg g$^{-1}$) | $R^2$ | $k_2$ (g mg$^{-1}$ min$^{-1}$) | $q_e$ (mg g$^{-1}$) | $R^2$ |
| M-UW | $8.13 \times 10^{-5}$ | 36.28 | 0.91471 | $7.77 \times 10^{-6}$ | 83.13 | 0.98581 |
| M-SW | $8.76 \times 10^{-5}$ | 46.08 | 0.91245 | $5.81 \times 10^{-5}$ | 73.69 | 0.99984 |
| MAUW-UW | $7.66 \times 10^{-5}$ | 47.74 | 0.84476 | $1.15 \times 10^{-5}$ | 77.82 | 0.9980 |
| MAUW-SW | $10.07 \times 10^{-5}$ | 69.28 | 0.91895 | $6.61 \times 10^{-5}$ | 72.52 | 0.99563 |
| MASW-UW | $6.38 \times 10^{-5}$ | 45.74 | 0.83063 | $1.58 \times 10^{-5}$ | 76.16 | 0.99527 |
| MASW-SW | $9.95 \times 10^{-5}$ | 64.39 | 0.95022 | $2.91 \times 10^{-6}$ | 95.06 | 0.98098 |

Mostrar os resultados de cinética e dar ênfase a suposição de que há mais de um processo de adsorção ocorrendo simultaneamente.
M-UW = histidine dissolved in ultrapure water, and adsorbed on montmorillonite; M-SW = histidine dissolved in seawater 4.0 (10%), and adsorbed on montmorillonite; MAUW-UW = histidine dissolved in ultrapure water, and adsorbed on modified montmorillonite with adenine in ultrapure water; MAUW-SW – histidine dissolved in seawater 4.0 (10%), and adsorbed on montmorillonite modified with adenine in ultrapure water; MASW-UW – histidine dissolved in ultrapure water, and adsorbed on montmorillonite modified with adenine in seawater 4.0 (10%); MASW-SW - histidine dissolved in seawater 4.0 (10%), and adsorbed on montmorillonite modified with adenine in seawater 4.0 (10%).

there is competition among histidine, adenine and seawater ions for the adsorption montmorillonite sites. For histidine adsorption onto the mineral, where there is no pre-adsorbed adenine or where the reaction does not occur in seawater solution, histidine would have more sites available to adsorb. Thus, higher adsorption onto the mineral would be expected.

For range 3, data did not fit in the pseudo-first-order or in the pseudo-second-order models (Fig. 4). For all experiments of this range, the correlation factor was less than 0.6 (data not shown).

For range 4, the data fitted well in the pseudo-second-order model (Table 3). Assuming that the adsorption reaction relative to the pseudo-first-order model (range 2) reached equilibrium after the transition phase (range 3), histidine is now binding to the mineral. The pseudo-second-order model assumes that the adsorption reaction is a chemical with a stronger interaction between the adsorbent and mineral surface (Largitte and Pasquier, 2016). Apparently, the kinetic mechanism is summed up by an initial charge attraction, hindered by positive charges from the seawater ions and pre-adsorbed adenine. From the moment that the active sites of the mineral are occupied by histidine molecules, this amino acid begins to adsorb onto the mineral in a different and slower way. This fact is recognized because all experiments carried out in seawater have a lower initial adsorption ratio, but with a higher reaction rate, proven by obtaining a kinetic constant '*k*' (Table 3) (Boyd *et al.*, 1947; Yasunaga and Ikeda, 1987).

Histidine adsorption onto negatively charged aluminosilicate shows a different adsorption mechanism. The first step is characterized by $NH_3^+$ histidine group interaction with negative mineral layers. This step is probably a cooperative adsorption of octa and tetramers histidine clusters onto the montmorillonite interlayer by an electrostatic interaction (Butyrskaya *et al.*, 2019). After many hours, reorganized clusters decrease the carboxylic repulsion with the mineral layer and an adapted system shows a hydrogen bond type interaction between histidine and montmorillonite (Butyrskaya *et al.*, 2019; Kotova *et al.*, 2020). Thus, literature data are in agreement with the experimental results: the first kinetic step is a histidine cluster outer-sphere interaction with montmorillonite while the second step is hydrogen bond formation by system reorganization.

## Adsorption isotherms

For a better understanding of the adsorption mechanism, adsorption isotherms were constructed using two different time ranges (Table 4). The first range used was 60 min after the solution was in contact with mineral and the second range was 10 080 min. The first range was chosen in order to better understand how adsorption occurs in the fastest step, and so that there was no adsorption mechanism overlap with other time ranges. The second range was chosen, in order to observe the reaction completely. Table 4 shows the non-linear regression coefficients ($R^2$) of Langmuir, Freundlich and SIP (Langmuir–Freundlich) models for each mineral and the temperature used in the two experimental time ranges. Figure 5 shows all experimental isotherms with the respective mathematical model as colour lines.

The SIP model showed the best fit for the first time range (60 min), while the second time range (10 080 min) fits the Langmuir model (Table 4). However, non-linear regression coefficients were very close to all models (Table 4). This is an indication that two distinct adsorption mechanisms can occur: homogeneously and with monolayer formation just like the Langmuir model, or heterogeneously according to the Freundlich model. Thus, the data showed that the adsorption mechanism is very sensitive to concentration and temperature. In addition, for time 10 080 min, data fits are close to the Langmuir model, meaning that montmorillonite has specific adsorption sites for histidine.

In general, when the temperature increased, the $Q_{max}$ values for the 60 min increased, while the 10 080 min showed an inverse trend (Table 5). For both times, MASW-SW showed the lowest $Q_{max}$ values and MASW-UW the highest $Q_{max}$ values (Table 5). Therefore, seawater salts have a negative effect on the adsorption of histidine onto montmorillonite. Also, for the MAUW-UW sample at 60 min, pre-adsorbed adenine decreased the adsorption of histidine when compared to M-UW sample (Table 5). However, at 10 080 min, the MAUW-UW sample showed high adsorption of histidine than the M-UW sample (Table 5). Probably, for a longer period of time, histidine reached to more energetic sites of montmorillonite, where adenine did not adsorb.

An essential characteristic of the Langmuir isotherm can be expressed by the separation factor ($R_L$), which predicts how favourable the reaction is. The values of $R_L > 1$ indicate that

**Table 4.** Non-linear regression coefficients ($R^2$) of Langmuir, Freundlich and SIP (Langmuir–Freundlich) models in the two experimental time ranges, at different temperatures

| Sample | Model | 0–60 min | | | 0–10 080 min | | |
|---|---|---|---|---|---|---|---|
| | | Temperature (℃) | | | | | |
| | | 20 | 35 | 50 | 20 | 35 | 50 |
| M-UW | Langmuir | 0.9874 | 0.9620 | 0.9765 | **0.9271** | **0.9723** | **0.9169** |
| | Freudlich | 0.9893 | 0.9629 | 0.9921 | 0.9119 | 0.9640 | 0.8822 |
| | SIPs | **0.9935** | **0.9485** | **0.9920** | 0.9119 | 0.9629 | 0.8758 |
| M-SW | Langmuir | 0.9809 | 0.9687 | 0.9713 | **0.9494** | **0.9262** | **0.9702** |
| | Freudlich | 0.9791 | 0.9704 | 0.9804 | 0.9489 | 0.9072 | 0.9225 |
| | SIPs | **0.9926** | **0.6784** | **0.9638** | 0.9226 | 0.9114 | 0.9797 |
| MAUW-UW | Langmuir | 0.9914 | 0.8992 | 0.9446 | **0.9130** | **0.9382** | **0.9264** |
| | Freudlich | 0.9873 | 0.9270 | 0.9674 | 0.8287 | 0.8440 | 0.8277 |
| | SIPs | **0.9926** | **0.9336** | **0.9638** | 0.9029 | 0.9356 | 0.9086 |
| MAUW-SW | Langmuir | 0.9655 | 0.9777 | 0.8236 | **0.9454** | **0.9469** | **0.9139** |
| | Freudlich | 0.9616 | 0.9778 | 0.8504 | 0.7826 | 0.9219 | 0.8955 |
| | SIPs | **0.9899** | **0.9629** | **0.9386** | 0.8908 | 0.9215 | 0.8765 |
| MASW-UW | Langmuir | 0.9871 | 0.9999 | 0.9774 | **0.9195** | **0.9243** | **0.9702** |
| | Freudlich | 0.9883 | 0.9998 | 0.9890 | 0.8865 | 0.8975 | 0.9325 |
| | SIPs | **0.9925** | **0.9999** | **0.9899** | 0.8898 | 0.8708 | 0.9698 |
| MASW-SW | Langmuir | 0.9204 | 0.9663 | 0.9534 | **0.9027** | **0.9137** | **0.8462** |
| | Freudlich | 0.9574 | 0.9411 | 0.9561 | 0.8618 | 0.8943 | 0.8462 |
| | SIPs | **0.9539** | **0.9857** | **0.9689** | 0.8673 | 0.8954 | 0.9147 |

M-UW = histidine dissolved in ultrapure water, and adsorbed on montmorillonite; M-SW = histidine dissolved in seawater 4.0 (10%), and adsorbed on montmorillonite; MAUW-UW = Histidine dissolved in ultrapure water, and adsorbed on modified montmorillonite with adenine in ultrapure water; MAUW-SW – histidine dissolved in seawater 4.0 (10%), and adsorbed on montmorillonite modified with adenine in ultrapure water; MASW-UW – histidine dissolved in ultrapure water, and adsorbed on montmorillonite modified with adenine in seawater 4.0 (10%); MASW-SW – histidine dissolved in seawater 4.0 (10%), and adsorbed on montmorillonite modified with adenine in seawater 4.0 (10%). Bold values are the best non-linear regression coefficients ($R^2$) obtained.

the process is unfavourable, $R_L = 1$ indicates a linear isotherm, $0 < R_L < 1$ indicates that the process is favourable and $R_L = 0$ indicates that the process is irreversible. Tables 1S and 2S (See supplementary materials) show the $R_L$ values close to 1 at a lower histidine concentration. Higher histidine concentrations show $R_L$ close to 0.5 indicating a greater tendency to an adsorption reaction (Ferrero, 2010; Dotto *et al.*, 2011). These data demonstrate that the system is sensitive to the histidine concentration and the adsorption is favoured by the histidine concentration increase. For all histidine concentrations, the $R_L$ values from the second time isotherms (10 080 min) were lower than 0.5, indicating a more favourable reaction (Table 2S).

Kotova *et al.* showed that the adsorption of histidine onto clinoptilolite, a negatively charged aluminosilicate similar to montmorillonite, occurs through the formation of a monolayer due to the electrostatic interaction between the amino group ($NH_3^+$) and negative sites of the mineral. The authors also observed repulsion between the carboxylic groups of the amino acid and the aluminium–oxygen groups with a negative charge. However, over time, this repulsion is minimized, and histidine starts to interact with the mineral also via hydrogen bonding (Kotova, *et al.*, 2020). As observed by Kotova *et al.*, two distinct histidine-montmorillonite adsorption times characterize the reorganization of the histidine adsorption system: the first

(60 min), a polymolecular layer (SIPs model) and the second, over longer times (10 080 min) a monolayer (Langmuir model).

### Thermodynamic measurements

From isotherm data and extrapolating the graphs of $Q_e/C_{eq}$ versus $Q_e$ on the *y*-axis, it is possible to calculate $K_{eq-}$, the equilibrium constant values of the adsorption reaction (Table 6). Gibbs energy and Van't Hoff equations and equilibrium constant values were used to calculate the thermodynamic parameters (Table 6) (Dotto *et al.*, 2011). Briefly, for the first time range (60 min), the adsorption was non-spontaneous and for the second time range (10 080 min), in all experiments, the adsorptions were spontaneous and guided by an enthalpy (Table 6).

Analysing the data of the first-time range isotherms without pre-adsorbed adenine on the mineral, the reaction in ultrapure water is enthalpically favoured. As it is an adsorption reaction, the system's order increases, decreasing its entropy (Table 6). The seawater experiments without pre-adsorbed adenine showed an opposite trend, since entropy increases, and although it was negative, it was higher than ultrapure water experiments. Seawater ions are hydrated and release water when adsorbed, releasing this hydration sphere and disordering the system. The interaction of seawater ions with minerals shows an endothermic process.
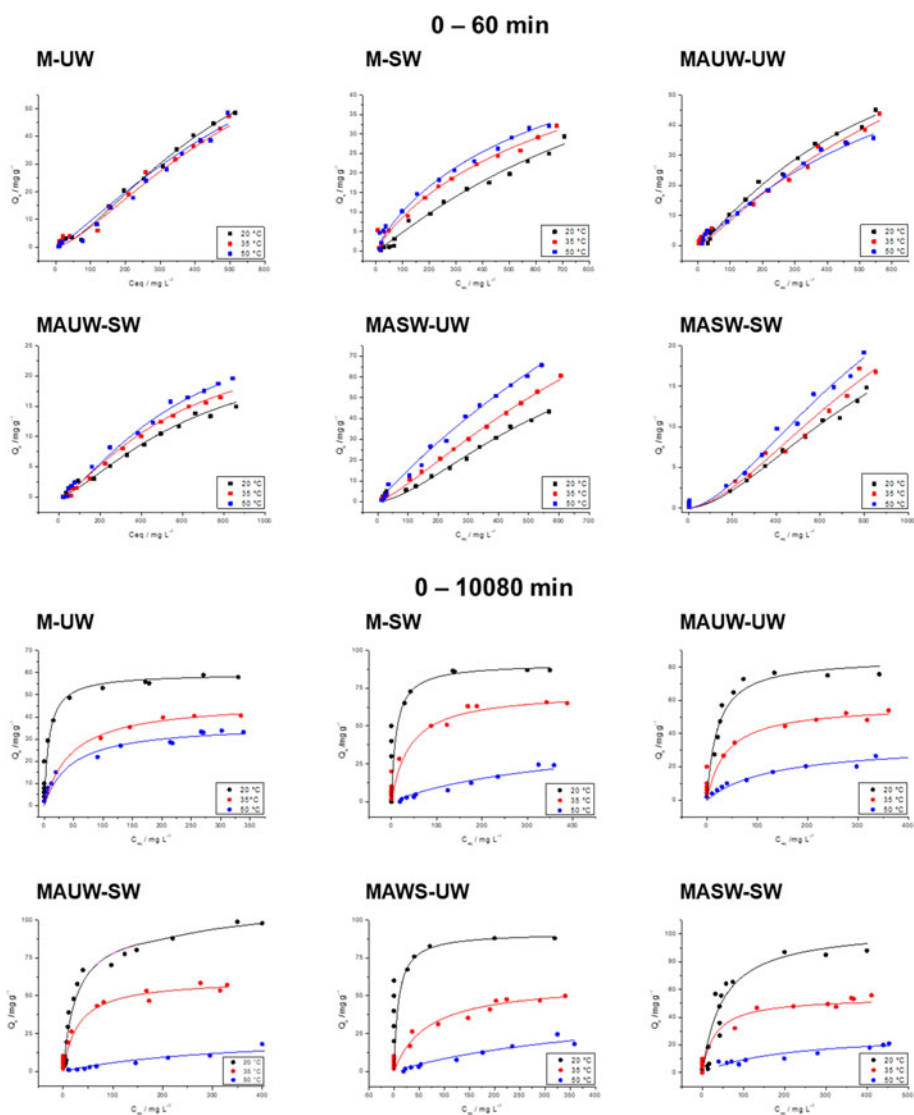
**0 – 60 min**



**0 – 10080 min**



**Fig. 5.** Experimental points isotherms and respective mathematical model colour lines of histidine adsorption onto mineral samples and solutions at different times. M-UW = histidine dissolved in ultrapure water, and adsorbed on montmorillonite; M-SW = histidine dissolved in seawater 4.0 (10%), and adsorbed on montmorillonite; MAUW-UW = histidine dissolved in ultrapure water, and adsorbed on modified montmorillonite with adenine in ultrapure water; MAUW-SW – histidine dissolved in seawater 4.0 (10%), and adsorbed on montmorillonite modified with adenine in ultrapure water; MASW-UW – histidine dissolved in ultrapure water, and adsorbed on montmorillonite modified with adenine in seawater 4.0 (10%); MASW-SW – histidine dissolved in seawater 4.0 (10%), and adsorbed on montmorillonite modified with adenine in seawater 4.0 (10%).

For the second time range, all reactions are spontaneous ($\Delta G < 0$), exothermic ($\Delta H < 0$) and the system becomes high ordering ($\Delta S < 0$) (Table 6). Comparing the first and second time ranges, it is possible to see that time is critical for system assembly. As shown in kinetics measurements, after approximately 7200 min, the adsorption behaves differently, fitting the pseudo-second-order model, and assuming a chemical nature reaction, providing a stronger interaction between the mineral and histidine (Table 3). In other words, if the adsorption time is longer, adsorption can occur more effectively, providing better results. This fact shows that for this specific adsorption time had great importance for system equilibrium.

To elucidate all possible histidine-system interactions, four possible interactions can be used on a linear system with experimental thermodynamic parameters in order to measure the contribution of each interaction to the adsorption system. Assuming the possible interactions with histidine are histidine–mineral = A, histidine–seawater ions = B, histidine–pre-adsorbed adenine = C and histidine–pre-adsorbed seawater ions = D, and using Hess law, a linear system can be built (Table 2). For all isotherms, the results shown in Table 2 represent the individual contribution of possible interactions A, B, C and D.

A set of linear equations were used to calculate thermodynamic parameters and associate them with experimental data. Using Table 2 data, thermodynamic parameters and respective shifts were calculated (Table 7). The data show good correlations, except the last comparison when histidine adsorbed onto montmorillonite with pre-adsorbed adenine in seawater 4.0 Gy (Table 7). It is probable this adsorption involves more interactions, such as ion–ion and ion–adenine, leaving a more complex system. Therefore, enthalpy and entropy values (A, B, C and D) are correlated with the experimental values. These values provide a better understanding of each interaction studied, showing that the enthalpy and entropy of each adsorption vary according to the interactions involved. For example, comparing the adsorption of histidine in ultrapure water (M-UW) with histidine adsorption onto montmorillonite with pre-adsorbed adenine in ultrapure water (MAUW-UW), it is possible to observe that the adenine–histidine interaction does not contribute to thermodynamic parameters. This is not the same for B and D parameters, which showed a large contribution for total enthalpy and entropy. Thus, it can be concluded that seawater ions have a large influence on the adsorption process.

**Table 5.** Adsorption isotherm parameters for two experimental times range

| Sample | Temperature (°C) | 0–60 min SIPs model | | | 0–10 080 min Langmuir model | |
| --- | --- | --- | --- | --- | --- | --- |
| | | Parameters | | | | |
| | | $Q_{max}$ (mg g$^{-1}$) | $K_L$ (A.U.) | $n$ (A.U.) | $Q_{max}$ (mg g$^{-1}$) | $K_L$ (A.U.) |
| M-UW | 20 | 96.26 | 0.00199 | 1.512 | 59.88 | 0.11920 |
| | 35 | 100.01 | 0.00169 | 1.435 | 49.68 | 0.05777 |
| | 50 | 120.00 | 0.00131 | 1.210 | 36.77 | 0.02225 |
| M-SW | 20 | 70.77 | 0.00093 | 1.104 | 91.19 | 0.09150 |
| | 35 | 72.85 | 0.00106 | 0.916 | 72.97 | 0.02456 |
| | 50 | 80.11 | 0.00106 | 0.901 | 45.57 | 0.00243 |
| MAUW-UW | 20 | 85.66 | 0.00186 | 1.179 | 85.47 | 0.04860 |
| | 35 | 97.47 | 0.00139 | 1.200 | 57.24 | 0.02610 |
| | 50 | 84.71 | 0.00149 | 1.100 | 34.01 | 0.00756 |
| MAUW-SW | 20 | 34.39 | 0.00096 | 1.164 | 98.97 | 0.03713 |
| | 35 | 36.79 | 0.00133 | 1.213 | 60.84 | 0.03305 |
| | 50 | 30.62 | 0.00175 | 1.641 | 29.97 | 0.00294 |
| MASW-UW | 20 | 92.21 | 0.00165 | 1.590 | 91.76 | 0.11070 |
| | 35 | 168.00 | 0.00102 | 1.274 | 59.07 | 0.01482 |
| | 50 | 303.6 | 0.00051 | 1.343 | 46.75 | 0.00218 |
| MASW-SW | 20 | 30.55 | 0.00113 | 1.726 | 104.7 | 0.02078 |
| | 35 | 39.56 | 0.00110 | 1.670 | 54.47 | 0.03242 |
| | 50 | 42.7 | 0.00108 | 1.650 | 28.80 | 0.00477 |

$Q_{max}$ = maximum adsorption capacity for histidine, $K_L$ = Langmuir constant and $n$ = Freundlich heterogeneity factor. M-UW = histidine dissolved in ultrapure water, and adsorbed on montmorillonite; M-SW = histidine dissolved in seawater 4.0 (10%), and adsorbed on montmorillonite; MAUW-UW = histidine dissolved in ultrapure water, and adsorbed on modified montmorillonite with adenine in ultrapure water; MAUW-SW – histidine dissolved in seawater 4.0 (10%), and adsorbed on montmorillonite modified with adenine in ultrapure water; MASW-UW – histidine dissolved in ultrapure water, and adsorbed on montmorillonite modified with adenine in seawater 4.0 (10%); MASW-SW – histidine dissolved in seawater 4.0 (10%), and adsorbed on montmorillonite modified with adenine in seawater 4.0 (10%).

Due to the large contribution of seawater ions to the histidine adsorption process, these ions were quantified after the adsorption experiments (Fig. 3). The largest amounts adsorbed, and, consequently, the highest thermodynamic contribution to the histidine adsorption system, are found in the magnesium and sulphate ions (Fig. 3). The interaction of histidine with montmorillonite occurs by an electrostatic interaction, which can lead to the adsorption of cations ($Mg^{2+}$) and anions ($SO_4^{2-}$) for a charge balance. The interaction with the mineral can be explained by a sequence of interactions. Initially, there is an interaction of magnesium with the mineral surface by an electrostatic attraction, the sulphate, in turn, adsorbs by an attraction with magnesium (Zaia et al., 2020). As the ions have a higher liability than histidine, system organization is quite slow, and therefore shows the stability after 7 days.

## Relevance for prebiotic chemistry

In general, adsorption experiments in prebiotic chemistry are performed in time ranges of 24 h. After 1 h, the adsorption of a substance onto a surface is usually almost completed. Naturally, quick adsorption of a substance onto a surface is very important in technological applications. However, in prebiotic chemistry, what difference does it make if adsorption takes 1 h, 1 day or even 1 year? We know that these experiments are models for understanding what could have happened on the prebiotic Earth. However, experiments with long adsorption times can provide a better idea of what occurred on the prebiotic Earth than experiments with short adsorption times. In addition, of all the suggestions made by Bernal, adsorption is the most important, because if the preconcentration of molecules does not occur, no other steps will occur (Bernal, 1951). The adsorption experiments described in this paper were performed over 1 week, which led to three important results: (1) at a longer period of time, pre-adsorbed adenine onto montmorillonite did not interfere in histidine adsorption, (2) the time of the adsorption changed the kinetics and thermodynamics of interaction of histidine with montmorillonite and (3) ions of artificial seawater have an effect on the adsorption of histidine onto montmorillonite. Firstly, it should be noted that the adsorption of histidine did not displace adenine from the montmorillonite. For short periods of time (60 min), the adsorption of histidine was slightly lower in the MAUW-UW sample than in the M-UW sample. In addition, comparing the adsorption of histidine in ultrapure water (M-UW) with histidine adsorption onto montmorillonite with pre-adsorbed adenine in ultrapure water (MAUW-UW), it is possible to observe that the adenine–histidine interaction does not contribute to thermodynamic parameters. The lack of

**Table 6.** Equilibrium constant and thermodynamic parameters for two time range isotherms

| Sample | Temperature (°C) | 0–60 min SIPs model | | | | 0–10 080 min Langmuir model | | | |
| | | $K_{eq}$ | $\Delta G$ (kJ mol$^{-1}$) | $\Delta H$ (kJ mol$^{-1}$) | $\Delta S$ (J mol$^{-1}$) | $K_{eq}$ | $\Delta G$ (kJ mol$^{-1}$) | $\Delta H$ (kJ mol$^{-1}$) | $\Delta S$ (J mol$^{-1}$) |
|---|---|---|---|---|---|---|---|---|---|
| M-UW | 20 | 0.1005 | 5.79 | −2.31 | −26.76 | 58.60 | −9.92 | −15.41 | −18.62 |
| | 35 | 0.0956 | 6.20 | | | 44.94 | −9.74 | | |
| | 50 | 0.0925 | 6.59 | | | 32.62 | −9.36 | | |
| M-SW | 20 | 0.0554 | 7.29 | 4.46 | −9.29 | 94.25 | −11.07 | −25.31 | −48.10 |
| | 35 | 0.0609 | 7.40 | | | 66.85 | −10.76 | | |
| | 50 | 0.0650 | 7.57 | | | 36.12 | −9.63 | | |
| MAUW-UW | 20 | 0.0796 | 6.37 | −2.79 | −30.30 | 79.12 | −10.65 | −16.12 | −18.60 |
| | 35 | 0.0743 | 6.87 | | | 58.35 | −10.41 | | |
| | 50 | 0.0720 | 7.28 | | | 42.84 | −10.09 | | |
| MAUW-SW | 20 | 0.0238 | 9.42 | 5.31 | −13.47 | 86.64 | −10.87 | −18.87 | −26.94 |
| | 35 | 0.0270 | 9.55 | | | 67.24 | −10.78 | | |
| | 50 | 0.0288 | 9.82 | | | 42.38 | −10.06 | | |
| MASW-UW | 20 | 0.0761 | 6.49 | 13.67 | 23.73 | 84.28 | −10.80 | −35.05 | −81.88 |
| | 35 | 0.1001 | 6.08 | | | 56.08 | −10.31 | | |
| | 50 | 0.1241 | 5.77 | | | 22.38 | −8.35 | | |
| MASW-SW | 20 | 0.0168 | 10.29 | 8.44 | −6.18 | 115.51 | −11.57 | −35.47 | −81.66 |
| | 35 | 0.0192 | 10.45 | | | 54.30 | −10.23 | | |
| | 50 | 0.0227 | 10.48 | | | 29.86 | −9.12 | | |

$\Delta G$ = Gibbs free energy; $\Delta H$ = enthalpy; $\Delta S$ = entropy; M-UW = histidine dissolved in ultrapure water, and adsorbed on montmorillonite; M-SW = histidine dissolved in seawater 4.0 (10%), and adsorbed on montmorillonite; MAUW-UW = histidine dissolved in ultrapure water, and adsorbed on modified montmorillonite with adenine in ultrapure water; MAUW-SW – histidine dissolved in seawater 4.0 (10%), and adsorbed on montmorillonite modified with adenine in ultrapure water; MASW-UW – histidine dissolved in ultrapure water, and adsorbed on montmorillonite modified with adenine in seawater 4.0 (10%); MASW-SW – histidine dissolved in seawater 4.0 (10%), and adsorbed on montmorillonite modified with adenine in seawater 4.0 (10%).

**Table 7.** Comparative board of experimental thermodynamic parameters and calculated parameters with linear system results

| Sample | 0–60 min | | | | | | 0–10 080 min | | | | | |
| | Exp. | | Calc. | | (Δ) | | Exp. | | Calc. | | (Δ) | |
| | $\Delta H$ | $\Delta S$ | $\Delta H$ | $\Delta S$ | $\Delta H$ | $\Delta S$ | $\Delta H$ | $\Delta S$ | $\Delta H$ | $\Delta S$ | $\Delta H$ | $\Delta S$ |
|---|---|---|---|---|---|---|---|---|---|---|---|---|
| M-UW | −2.3 | 26.8 | −2.3 | 26.8 | 0.0 | 0.0 | −15.41 | −18.62 | −15.41 | −18.62 | 0.0 | 0.0 |
| M-SW | 4.4 | −9.2 | 5.9 | −9.3 | 1.5 | 0.1 | −25.31 | −48.10 | −25.31 | −48.10 | 0.0 | 0.0 |
| MAUW-UW | −2.7 | 30.3 | −1.4 | 32.8 | 1.3 | 2.5 | −16.12 | −18.60 | −16.12 | −14.52 | 0.0 | 4.08 |
| MAUW-SW | 5.3 | 13.5 | 6.8 | 15.3 | 1.5 | 1.9 | −18.87 | −26.94 | −26.02 | −44.00 | 7.15 | 17.06 |
| MASW-UW | 13.6 | 23.7 | 14.9 | 21.2 | 1.3 | 2.5 | −35.05 | −81.88 | −32.72 | −69.24 | 2.33 | 12.64 |
| MASW-SW | 8.4 | −6.1 | 23.1 | 38.7 | 14.7 | 32.5 | −35.47 | −81.66 | −42.62 | −98.72 | 7.15 | 17.06 |

Δ represents the modular shifts for experimental and calculated results.
M-SW = histidine dissolved in seawater 4.0 (10%), and adsorbed on montmorillonite; MAUW-UW = histidine dissolved in ultrapure water, and adsorbed on modified montmorillonite with adenine in ultrapure water; MAUW-SW – histidine dissolved in seawater 4.0 (10%), and adsorbed on montmorillonite modified with adenine in ultrapure water; MASW-UW – histidine dissolved in ultrapure water, and adsorbed on montmorillonite modified with adenine in seawater 4.0 (10%); MASW-SW – histidine dissolved in seawater 4.0 (10%), and adsorbed on montmorillonite modified with adenine in seawater 4.0 (10%).

interference of adenine in the adsorption of histidine means that montmorillonite was able to adsorb both molecules. The implication for prebiotic chemistry is that different reactions could occur on the montmorillonite surface. We should remember that amino acids are linked to polymers that are catalysts and nucleic acid bases are linked to polymers that contain information (Darnell

*et al.*, 1990). Using a longer time for the adsorption of histidine onto montmorillonite showed that a thermodynamically unfavourable process in a short time becomes a thermodynamically favourable process in a long time. In addition, the kinetics of the reaction changed. These results are important for prebiotic chemistry because they give a better picture of what could have happened on the prebiotic Earth. Since most articles published in prebiotic chemistry do not take into account the effect of salts of seawater on the adsorption of molecules onto minerals (Zaia, 2012), this paper highlights this issue. Thus, the conditions used in this paper are probably more closely resemble the existing environment of the prebiotic Earth.

## Conclusion

In general, adsorption experiments under prebiotic chemistry conditions are carried out in a maximum time of 24 h. However, in the present work, the adsorption was studied for 7 days. After adsorbing adenine, montmorillonite also adsorbs histidine, showing that even though the nitrogenous base is already adsorbed, montmorillonite still has free adsorption sites. The two-time adsorption isotherms division showed that seawater 4.0 Gy ions influence the histidine adsorption, whether pre-adsorbed with adenine onto montmorillonite or in solution together with histidine. Thus, the seawater composition is extremely significant for prebiotic experiments. The one-hour adsorption isotherm data showed that although the adsorption is not favourable, it is sensitive to histidine concentration, probably due to the negative carboxylic charge of the histidine group and the mineral surface repulsion. Seven-day isotherms provided results of a favourable adsorption reaction (with negative $\Delta G$) and an organized system with low entropy, indicating that the system was reorganized by the hydrogen bond formation. Adenine, in general, has no significant thermodynamic relevance when present in adsorption experiments, unlike pre-adsorbed seawater ions, which, when present, contribute to adsorption and system reorganization according to thermodynamic parameters.

## References

Anizelli PR, Baú JPT, Gomes FP, da Costa ACS, Carneiro CEA, Zaia CTBV and Zaia DAM (2015) A prebiotic chemistry experiment on the adsorption of nucleic acids bases onto a natural zeolite. *Origins of Life and Evolution of Biospheres* 45, 289–306.

Anizelli PR, Baú JPT, Valezi DF, Canton LC, Carneiro CEA, Di Mauro E, da Costa ACS, Galante D, Braga AH, Rodrigues F, Coronas J, Casado-Coterillo C, Zaia CTBV and Zaia DAM (2016) Adenine interaction with and adsorption on Fe-ZSM-5 zeolites: a prebiotic chemistry study using different techniques. *Microporous and Mesoporous Materials* 226, 493–504.

Aufdenkampe AK, Hedges JI, Richey JE, Krusche AV and Llerena CA (2001) Sorptive fractionation of dissolved organic nitrogen and amino acids onto fine sediments within the Amazon Basin. *Limnology and Oceanography* 46, 1921–1935.

Basiuk VA (2002). Adsorption of biomolecules at silica. In Hubbard AT (ed). *Encyclopedia of Surface and Colloid Science*. Boca Raton, Florida: CRC-Press, p. 359.

Basiuk VA and Gromovoy TY (1996) Comparative study of amino acid adsorption on bare and octadecyl silica from water using high-performance liquid chromatography. *Colloids and Surfaces A: Physicochemical and Engineering Aspects* 118, 127–140.

Baú JPT, Carneiro CEA, de Souza Junior IG, de Souza CMD, da Costa ACS, di Mauro E, Zaia CTBV, Coronas J, Casado C, de Santana H and Zaia DAM (2012) Adsorption of adenine and thymine on zeolites: FT-IR and EPR spectroscopy and X-ray diffractometry and SEM studies. *Origins of Life and Evolution of Biospheres* 42, 19–29.

Ben-Taleb A, Vera P, Delgado AV and Gallardo V (1994) Electrokinetic studies of monodisperse hematite particles: effects of inorganic electrolytes and amino acids. *Materials Chemistry and Physics* 37, 68–75.

Benetoli LOB, de Souza CMD, da Silva KL, de Souza IG, de Santana H, Paesano A, da Costa ACS, Zaia CTBV and Zaia DAM (2007) Amino acid interaction with and adsorption on clays: FT-IR and Mössbauer spectroscopy and X-ray diffractometry investigations. *Origins of Life and Evolution of Biospheres* 37, 479–493.

Benetoli LOB, de Santana H, Zaia CTBV and Zaia DAM (2008) Adsorption of nucleic acid bases on clays: an investigation using Langmuir and Freundlich isotherms and FT-IR spectroscopy. *Monatshefte Für Chemie-Chemical Monthly* 139, 753–761.

Bera PP, Stein T, Head-Gordon M and Lee TJ (2017) Mechanisms of the formation of adenine, guanine, and their analogues in UV-irradiated mixed $NH_3:H_2O$ molecular ices containing purine. *Astrobiology* 17, 771–785.

Bernal JD (1951) *The physical basis of life*. London, UK: Routledge and Kegan Paul Ltd.

Boyd GE, Adamson AW and Myers LS (1947) The exchange adsorption of ions from aqueous solutions by organic zeolites. II. Kinetics. *Journal of the American Chemical Society* 69, 2836–2848.

Butyrskaya EV, Zapryagaev SA and Izmailova EA (2019) Cooperative model of the histidine and alanine adsorption on single-walled carbon nanotubes. *Carbon* 143, 276–287.

Carneiro CEA, de Santana H, Casado C, Coronas J and Zaia DAM (2011a) Adsorption of amino acids (Ala, Cys, His, Met) on zeolites: Fourier transform infrared and Raman spectroscopy investigations. *Astrobiology* 11, 409–418.

Carneiro CEA, Berndt G, de Junior IGS, de Souza CMD, Paesano A, da Costa ACS, di Mauro E, de Santana H, Zaia CTBV and Zaia DAM (2011b) Adsorption of adenine, cytosine, thymine, and uracil on sulfide-modified montmorillonite: FT-IR, Mössbauer and EPR spectroscopy and X-ray diffractometry studies. *Origins of Life and Evolution of Biospheres*. doi: 10.1007/s11084-011-9244-3.

Churchill H, Teng H and Hazen RM (2004) Correlation of pH-dependent surface interaction forces to amino acid adsorption: implications for the origin of life. *American Mineralogist* 89, 1048–1055.

Darnell J, Lodish D and Baltimore D (1990) *Molecular Cell Biology*. New York, USA: Scientific American Books, pp. 771–777.

Ding X and Henrichs SM (2002) Adsorption and desorption of proteins and polyamino acids by clay minerals and marine sediments. *Marine Chemistry* 77, 225–237.

Dotto GL, Vieira MLG, Gonçalves JO and Pinto LAA (2011) Remoção dos corantes azul brilhante, amarelo crepúsculo e amarelo tartrazina de soluções aquosas utilizando carvão ativado, terra ativada, terra diatomácea, quitina e quitosana: estudos de equilíbrio e termodinâmica. *Química Nova* 34, 1193–1199.

Farias APSF, Tadayozzi YS, Carneiro CEA and Zaia DAM (2014) Salinity and pH affect Na⁺-montmorillonite dissolution and amino acid adsorption: a prebiotic chemistry study. *International Journal of Astrobiology* 13, 259–270.

Farias APSF, Carneiro CEA, de Batista Fonseca IC, Zaia CTBV and Zaia DAM (2016) The adsorption of amino acids and cations onto goethite: a prebiotic chemistry experiment. *Amino Acids* 48, 1401–1412.

Ferrero F (2010) Adsorption of methylene blue on magnesium silicate: kinetics, equilibria and comparison with other adsorbents. *Journal of Environmental Sciences* 22, 467–473.

Ferris JP (1993) Catalysis and prebiotic RNA synthesis. *Origins of Life and Evolution of the Biosphere* 23, 307–315.

Ferris JP and Hagan Jr WJ (1984) HCN and chemical evolution: the possible role of cyano compounds in prebiotic synthesis. *Tetrahedron* 40, 1093–1120.

Ferris JP, Joshi PC, Edelson EH and Lawless JG (1978) HCN: a plausible source of purines, pyrimidines and amino acids on the primitive earth. *Journal of Molecular Evolution* **11**, 293–311.

Foo KY and Hameed BH (2010) Insights into the modeling of adsorption isotherm systems. *Chemical Engineering Journal* **156**, 2–10.

Fripiat J (1984) A.G. Cairns-Smith. Genetic Takeover and the Mineral Origins of Life. Cambridge University Press, 1982. 477 pp. Price £15.00. *Clay Minerals* **19**, 121–122.

Hardy PM (1985) Chapter 2: The protein amino acids. In Barret GC (ed). *Chemistry and Biochemistry of the Amino Acids*. London: Chapman and Hall, pp. 6–24.

Hazen RM, Papineau D, Bleeker W, Downs RT, Ferry JM, McCoy TJ, Sverjensky DA and Yang H (2008) Mineral evolution. *American Mineralogist* **93**, 1693–1720.

Hedges JI and Hare PE (1987) Amino acid adsorption by clay minerals in distilled water. *Geochimica et Cosmochimica Acta* **51**, 255–259.

Henrichs SM and Sugai SF (1993) Adsorption of amino acids and glucose by sediments of Resurrection Bay, Alaska, USA: functional group effects. *Geochimica et Cosmochimica Acta* **57**, 823–835. DOI: 10.1016/0016-7037 (93)90171-R.

Holm NG and Andersson E (2005) Hydrothermal simulation experiments as a tool for studies of the origin of life on earth and other terrestrial planets: a review. *Astrobiology* **5**, 444–460.

Jaber M, Georgelin T, Bazzi H, Costa-Torro F, Lambert JF, Bolbach G and Clodic G (2014) Selectivities in adsorption and peptidic condensation in the (arginine and glutamic acid)/montmorillonite clay system. *The Journal of Physical Chemistry C* **118**, 25447–25455.

Jackson TA (1971) Preferential polymerization and adsorption of L-optical isomers of amino acids relative to D-optical isomers on kaolinite templates. *Chemical Geology* **7**, 295–306.

Kotova DL, Krysanova TA and Vasil'eva SY (2020) Equilibrium sorption of histidine on clinoptilolite. *Colloid Journal* **82**, 284–287.

Lahav N (1994) Minerals and the origin of life – hypotheses and experiments in heterogeneous chemistry. *Heterogeneous Chemistry Reviews* **1**, 159–179.

Lahav N and Chang S (1976) The possible role of solid surface area in condensation reactions during chemical evolution: reevaluation. *Journal of Molecular Evolution* **8**, 357–380.

Lambert JF (2008) Adsorption and polymerization of amino acids on mineral surfaces: a review. *Origins of Life and Evolution of the Biosphere* **38**, 211–242.

Largitte L and Pasquier R (2016) A review of the kinetics adsorption models and their application to the adsorption of lead by an activated carbon. *Chemical Engineering Research and Design* **109**, 495–504.

Lazcano A and Miller SL (1996) The origin and early evolution of life: prebiotic chemistry, the pre-RNA world, and time. *Cell* **85**, 793–798.

Lee N, Sverjensky DA and Hazen RM (2014) Cooperative and competitive adsorption of amino acids with $Ca^{2+}$ on rutile ($\alpha$-$TiO_2$). *Environmental Science & Technology* **48**, 9358–9365.

Li F, Fitz D, Fraser DG and Rode BM (2010) Arginine in the salt-induced peptide formation reaction: enantioselectivity facilitated by glycine, l- and d-histidine. *Amino Acids* **39**, 579–585.

Lowe CU, Rees MW and Markham R (1963) Synthesis of complex organic compounds from simple precursors: formation of amino acids, amino acid polymers, fatty acids and purines from ammonium cyanide. *Nature* **199**, 219–222.

Martins Z, Botta O, Fogel ML, Sephton MA, Glavin DP, Watson JS, Dworkin JP, Schwartz AW and Ehrenfreund P (2008) Extraterrestrial nucleobases in the Murchison meteorite. *Earth and Planetary Science Letters* **270**, 130–136.

Montluçon DB and Lee C (2001) Factors affecting lysine sorption in a coastal sediment. *Organic Geochemistry* **32**, 933–942.

Paecht-Horowitz M (1977) The mechanism of clay catalyzed polymerization of amino acid adenylates. *Biosystems* **9**, 93–98.

Perezgasga L, Serrato-Díaz A, Negrón-Mendoza A, Gal'N LDP and Mosqueira FG (2005) Sites of adsorption of adenine, uracil, and their corresponding derivatives on sodium montmorillonite. *Origins of Life and Evolution of Biospheres* **35**, 91–110.

Plankensteiner K, Reiner H and Rode BM (2006) Amino acids on the rampant primordial earth: electric discharges and the hot salty ocean. *Molecular Diversity* **10**, 3–7.

Rao M, Odom DG and Oró J (1980) Clays in prebiological chemistry. *Journal of Molecular Evolution* **15**, 317–331.

Roy D, Najafian K and von Rague Schleyer P (2017) Chemical evolution: the mechanism of the formation of adenine under prebiotic conditions. *Proceedings of the National Academy of Sciences U.S.A.* **104**, 17272–17277.

Schoonen M, Smirnov A and Cohn C (2004) A perspective on the role of minerals in prebiotic synthesis. *AMBIO: A Journal of the Human Environment* **33**, 539–551.

Shen C, Yang L, Miller SL and Oró J (1990) Prebiotic synthesis of histidine. *Journal of Molecular Evolution* **31**, 167–174.

Stoks PG and Schwartz AW (1979) *Nature* **282**, 709–710.

Suzuki T, Yano T, Hara M and Ebisuzaki T (2018) Cysteine and cystine adsorption on FeS2(100). *Surface Science* **674**, 6–12.

Tanaka H, Miyajima K, Nakagaki M and Shimabayashi S (1989) Interactions of aspartic acid, alanine and lysine with hydroxyapatite. *Chemical & Pharmaceutical Bulletin* **37**, 2897–2901.

Uehara G (1979) Mineral–Chemical properties of oxisols. In International Soil Classification Workshop, Volume 2; Soil Survey Division-Land Development Department: Bangkok, Thailand, pp. 45–46.

Vieira AP, Berndt G, de Souza Junior IG, Di Mauro E Jr, Paesano A, de Santana H, da Costa ACS, Zaia CTBV and Zaia DAM (2011) Adsorption of cysteine on hematite, magnetite and ferrihydrite: FT-IR, Mössbauer, EPR spectroscopy and X-ray diffractometry studies. *Amino Acids* **40**, 205–214.

Villafañe-Barajas SA, Baú JPT, Colín-García M, Negrón-Mendoza A, Heredia-Barbero A, Pi-Puig T and Zaia DAM (2018) Salinity effects on the adsorption of nucleic acid compounds on Na-montmorillonite: a prebiotic chemistry experiment. *Origins of Life and Evolution of Biospheres* **48**, 181–200.

Winter D and Zubay G (1995) Binding of adenine and adenine-related compounds to the clay montmorillonite and the mineral hydroxylapatite. *Origins of Life and Evolution of the Biosphere* **25**, 61–81.

Yasunaga T and Ikeda T. (1987) Adsorption-Desorption Kinetics at the Metal-Oxide-Solution Interface Studied by Relaxation Methods. In *Geochemical Processes at Mineral Surfaces, ACS Symposium Series*, vol. **323**, pp. 230–250.

Zaia DAM (2012) Adsorption of amino acids and nucleic acid bases onto minerals: a few suggestions for prebiotic chemistry experiments. *International Journal of Astrobiology* **11**, 229–234.

Zaia DAM, Vieira HJ and Zaia CTBV (2002) Adsorption of L-amino acids on sea sand. *Journal of the Brazilian Chemical Society* **13**, 679–681.

Zaia DAM, de Carvalho PCG, Samulewski RB, de Carvalho Pereira R and Zaia CTBV (2020) Unexpected thiocyanate adsorption onto ferrihydrite under prebiotic chemistry conditions. *Origins of Life and Evolution of Biospheres* **50**, 57–76.

Zenebon O, Pascuet NS and Tiglea P (2008) Minerais e contaminantes inorgânicos. In Oldair Zenebon, Neus Sadocco Pascuet and Paulo Tiglea (eds). *Métodos Físico-Químicos Para Análise de Alimentos*, 4th edition edn, São Paulo-SP, Brasil: Editora do Instituto Adolfo Lutz, pp. 735–754.